Quantitative 2D-Mixture Fraction Imaging Inside An Internal Combustion Engine Using Aceton-Fluorescence

D.Wolff, V.Beushausen, H.Schlüter, P.Andresen,
W.Hentschel*, P.Manz* and S.Arndt**

Laser-Laboratorium Göttingen
Postfach 2619, D-37077 Göttingen
Germany
* *Volkswagen AG*
** *Robert Bosch GmbH*

ABSTRACT

Planar Laser Induced Fluorescence has been used to obtain 2D-fuel-distribution-images and λ-value maps inside a cylinder of a modified mass production four-cylinder SI-engine. For the investigations special stress was layed on the analysis of the influence of the variation of engine parameters on fuel- and λ-value distribution.

For visualization of the non fluorescent iso-octane fuel the fluorescent tracer substance acetone was homogeneously premixed with the fuel. For different engine parameters (time of injection during the engine cycle, overall λ-value, exhaust gas recirculation (EGR)) both snap shots (single laser shot images) and averaged images of 2D-fuel distributions were detected for a variety of different crank angles. The investigations yield a) instantaneous qualitative detection of planar fuel distributions and the progress of turbulent mixing formation in dependance on the engine parameters, b) averaged 2D-fuel distributions for a series of single crank angles using on-chip averaging and c) instantaneous quantitative measure of planar λ-value- distribution (λ-value maps) using simple calibration and correction procedures.

INTRODUCTION

During the past few years a rapid development of nonintrusive measurement techniques for application in technical turbulent combustion systems took place. Especially new powerful UV-lasers in combination with modern camera technology and optical accessibility of the combustion systems facilitated new insights in mechanisms determining the course of combustion. 2D-LIF, LIPF, Raman- and Rayleigh scattering were already succesfully applied e.g. for visualization and density measurements of different combustion relevant molecular species (OH, O_2, NO, fuel ...) [1-6], temperature measurements in combustion gases and flame front imaging in engines [7]. Especially spontaneous Raman scattering is used to measure the in-cylinder equivalence ratio and residual gas content with high precision directly via the densities of fuel, O_2, N_2 and H_2O in single cycles [8]. The work demonstrates that cyclic variations of these two parameters have a strong influence on cycle-by-cycle variations of the indicated work (IMEP). The 2D investigation of mixing processes and λ-values inside the cylinder of real SI engines usually raised problems because the application of fluorescing tracer substances suffers from hostile temperature and pressure conditions. Recently some interesting work concerning these problems were carried out [8-13]. Using the tracer diethyl ketone Vannobel et al. concluded that fuel is homogeneously distributed after completion of the intake process [13]. The present work however demonstrates that this result has to be due to poor dynamic range of the detection system used. In this work acetone is used as fuel tracer and it is shown that strong inhomogeneous fuel distribution and spatially fluctuating λ-values are detectable up to TDC in the compression stroke using 12 bit intensified CCD-cameras. Measurement object was a modified mass production four cylinder in line engine from VOLKSWAGEN which also allowed the investigation of influences resulting from variations of engine parameters on fuel- and λ-value distribution.

EXPERIMENTAL SETUP

The investigations were carried out in one cylinder of a mass production four cylinder SI-engine supplied by VOLKSWAGEN AG. The engine was modified to facilitate optical access by placing two quartz windows (2x2mm²) in the cylinder walls near the cylinder head for laser beam entrance and one 50mm diameter quartz window in the elongated piston for observation purposes (see **fig.1**). Some important engine data are displayed in **table 1**. The engine is equipped with a mass production BOSCH port fuel injection system with an injector in the intake port of each cylinder. The pulsed fuel spray is directed towards the intake valve. Several engine parameters can be changed and controlled externally, e.g. engine speed, load, λ-value (cycle-averaged measurement by a lambda probe (Bosch LSM11 0258104001) located in the exhaust port of the measurement cylinder), time of fuel injection during the engine cycle and exhaust gas recirculation (EGR). The parameters used for the measurements presented below are indicated in the table. Instead of air/fuel equivalence ratio in the following the expression λ-value is used. The assignment of λ-values is as followes:

$\lambda < 1$	rich
$\lambda = 1$	stoichiometric
$\lambda > 1$	lean

More details about the experimental setup are described elsewhere [4]. In the next section it is shown that the external variation of the engine parameters time of fuel injection, equivalence ratio and exhaust gas recirculation has a tremendous effect on engine behaviour. For every parameter two cases are compared below:

Time of injection: a) during intake stroke ≡ "late" (around 90°CA after TDC)
b) during compression stroke ≡ "early" (around 90°CA bef. TDC)

Equivalence ratio: a) stoichiometric (λ=1.0)
b) fuel rich (λ=0.8)

EGR: a) without
b) 12% recirculation

The detection system

For excitation broadband XeCl-excimer laser radiation was used. The laser light was formed to a light sheet (0.5x20mm²) and coupled into the cylinder through two thick silica windows (**fig.1**). The fluorescence left the cylinder perpendicular to excitation through a 50mm diameter silica window in the piston and was detected by a 12 bit intensified CCD-camera (LaVision). The resulting digital image was instantaneously displayed on a monitor and stored in PC-memory for subsequent data evaluation.

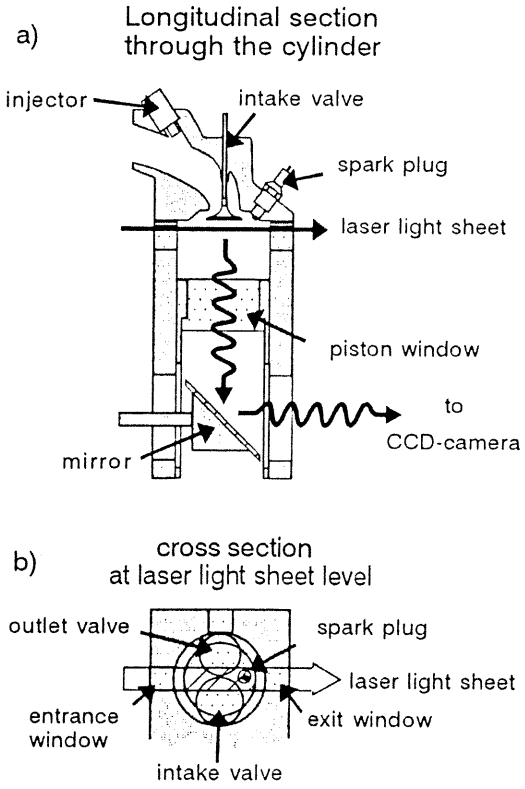

Fig.1: Longitudinal cylinder section (a) and horizontal cylinder section at laser sheet position (b). The shaded area in (b) represents the position of the detected fuel distribution images inside the cylinder.

Table 1: Engine Description and Operating Conditions

Number of cylinders:	4
Bore (mm):	81
Stroke (mm):	86.4
Compression Ratio:	6.5
Displacement Volume (L):	1.8
Fuel Injection System:	multipoint PFI
Engine Speed (r.p.m.):	1500
Torque (Nm):	40
Coolant Temperature:	80°C

RESULTS AND DISCUSSION

Figs. 2-5 show images of planar fuel distributions for different engine parameters (see above) and three different crank angles (CA). In **Fig.2** fuel distributions for intake port fuel injection during the compression stroke (around crank angle 90°CA before TDC) are presented. The left column of the figure shows snap shots of the distribution for three different crank angles. The origin of the crank angle scale is fixed at ignition TDC. In the right column cycle averaged distributions (20 cycles) at the same crank angles are shown.

The relative fuel densities presented are coded via a grey scale indicated at the right. For better presentation and to facilitate compareability of fuel distribution structures of images with strongly different signal intensities the grey values are chosen in a way that the highest intensity of every image correspond to the color white of the grey scale. In practice this means that the signal intensities (fuel densities) of the images of the first two crank angles were multiplied by a factor F given at the right side of each image.

As expected the snap shot image at 524°CA shows a cloudy, extremely inhomogeneous fuel distribution with some steep gradients indicating the turbulent mixing of fuel and air during the intake stroke. A higher fuel concentration is detectable in the lower part of the image where the intake valve is located (see **fig.1**). This here only suggested structure is clearly developed in the cycle averaged image (20 cycles) in the right column of the figure. Through the averaging process the cyclic fluctuations of fuel density disappear and a spatially fixed fuel distribution structure is formed. The development of this fuel rich structure below the intake valve is due to vortices formed by the incoming stream of fuel and air.

As the snap shot image taken in the compression stroke 20°CA before ignition (664°CA) clearly demonstrates the mixing of fuel and air is not complete. Even at this very late position in the compression stroke a cloudy structure of fuel rich and lean areas is detectable (see also λ-map in **fig.6**). As expected the averaged distribution at the right does not show this structure any more but a steady increase of relative fuel density from the left to the right (spark plug position) is clearly detectable. Since this image is also averaged over 20 different working cycles of the engine the measured data imply that at the present CA and for the present engine configuration on average higher fuel densities appear in the surroundings of the spark plug.

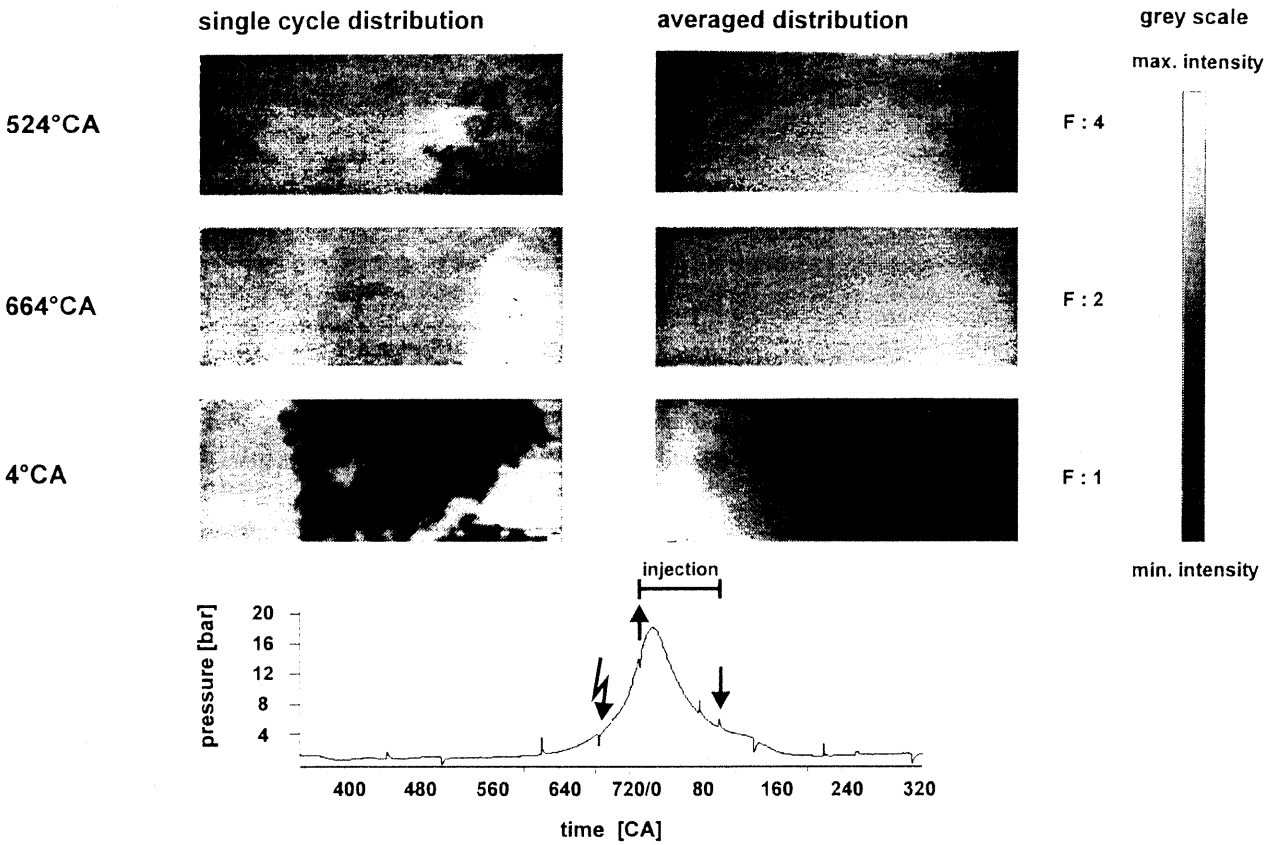

Fig. 2 : Fuel distributions after fuel injection during combustion stroke and averaged pressure trace. Operating conditions: 1400 RPM, torque: 40 Nm, lambda: 1.0.

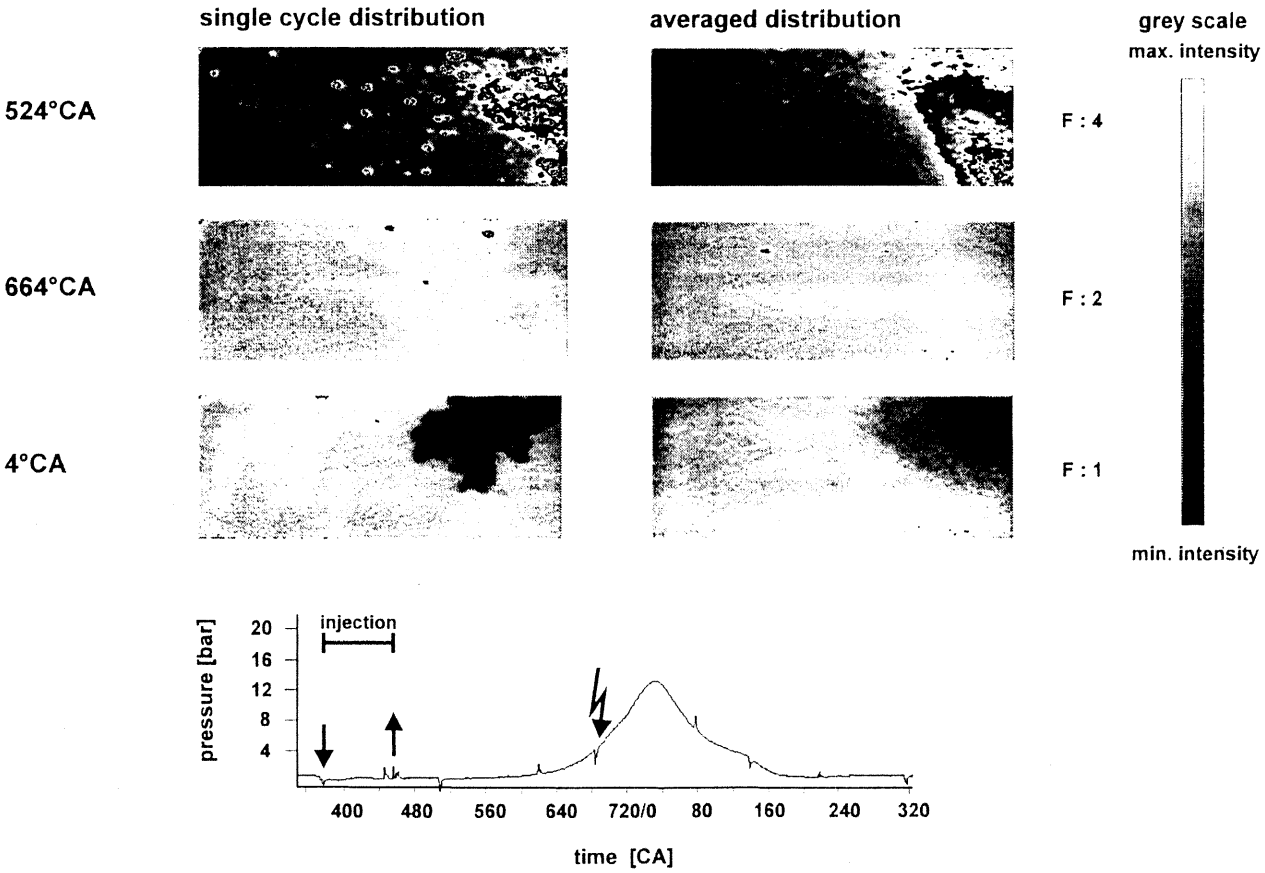

Fig. 3 : Fuel distributions after fuel injection during inlet stroke and averaged pressure trace. Operating conditions: 1400 RPM, torque: 40 Nm, lambda: 1.0.

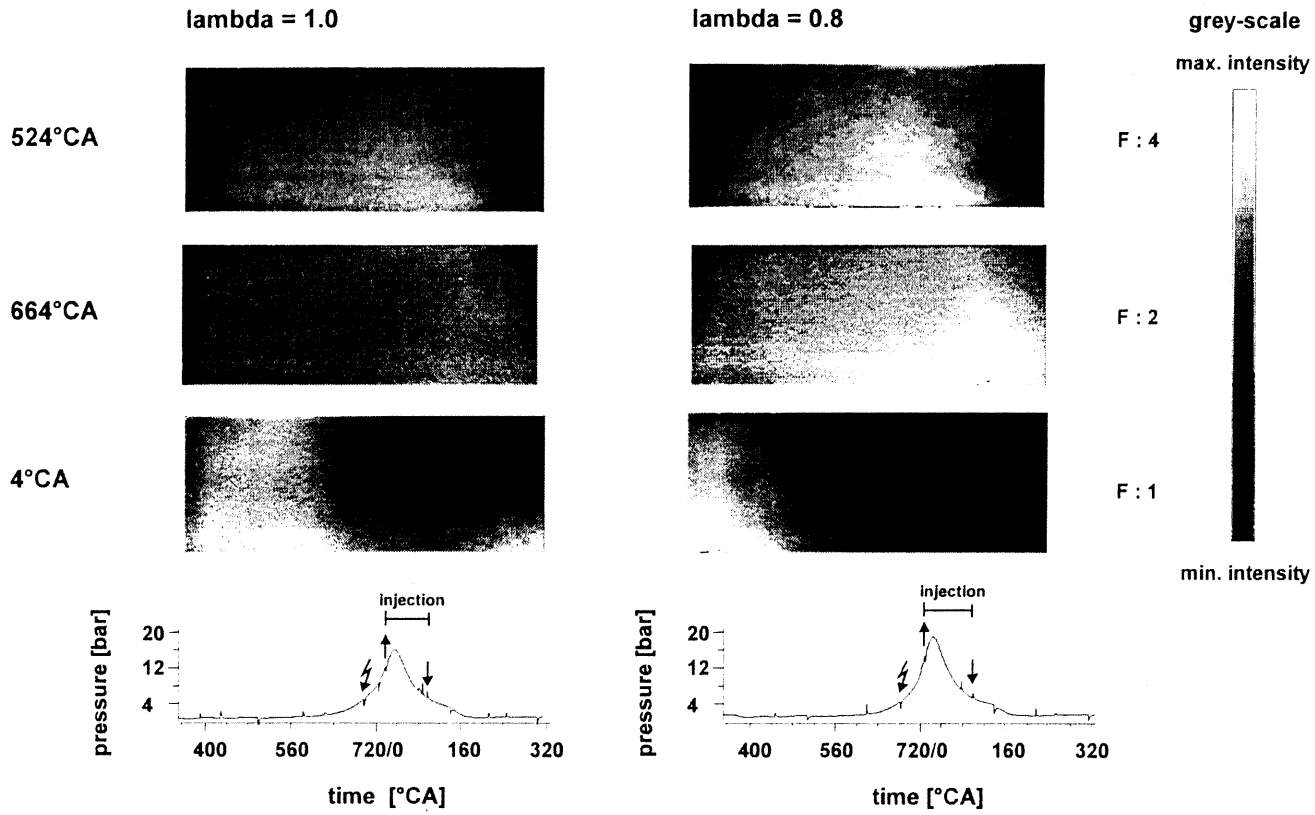

Fig. 4: Averaged fuel distributions and pressure curves showing the influence of different overall lambda-values. Operating conditions: 1400 RPM, torque: 40 Nm, no EGR.

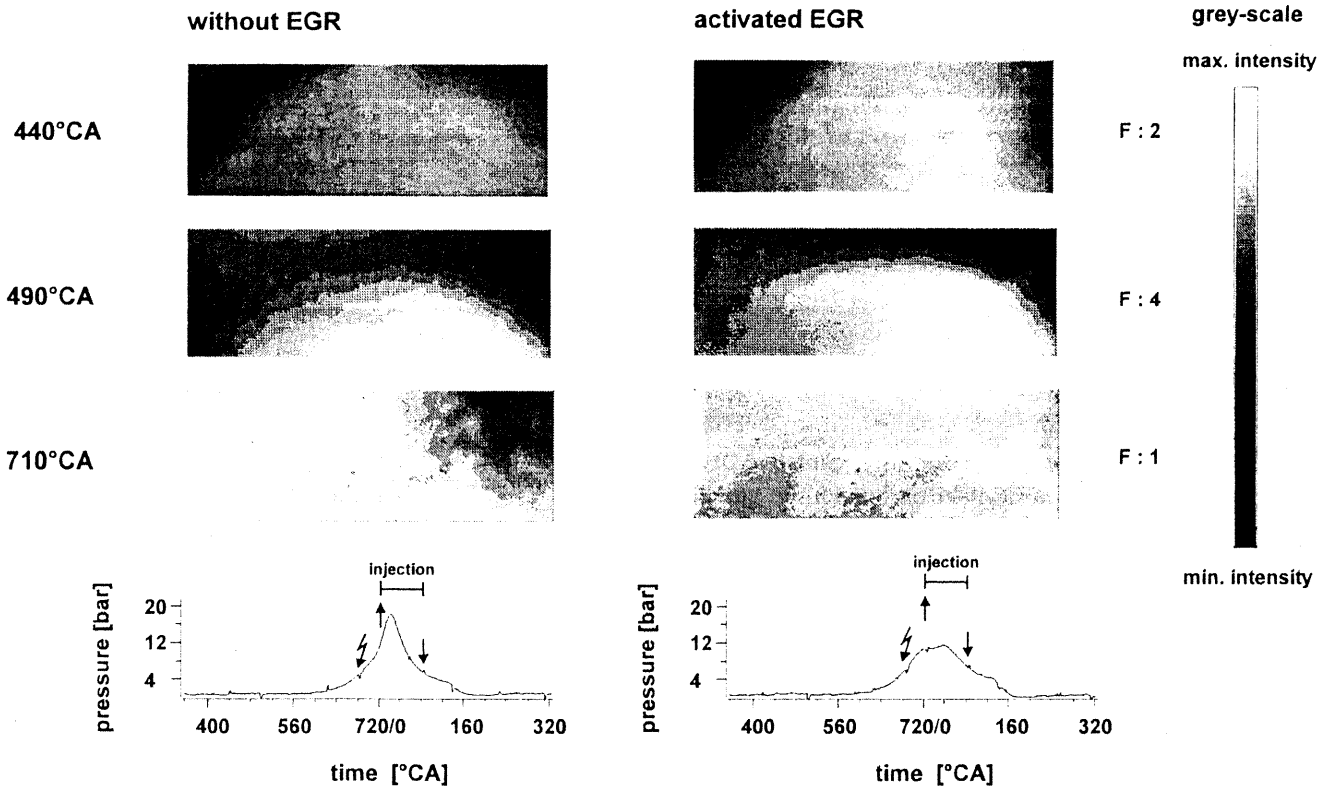

Fig. 5: Averaged fuel distributions and pressure curves showing the influence of exhaust gas recirculation (EGR). Operating conditions: 1400 RPM, torque: 40Nm, lambda: 1.0.

The last snap shot image in fig.2 is taken nearly 40°CA after ignition at 4°CA. The black area in the middle represents the position of the burnt or still burning air/fuel mixture. The strongly structured flame front is indicated by the steep gradient between high fuel density in the unburned region and the not fluorescing area of burnt or burning gas. In the cycle averaged image this gradient is more gentle due to averaging of the cyclic variations of flame front positions.

Below the images in fig.2 the progress of in-cylinder pressure averaged over 20 cycles is shown. The small spikes on top of the pressure trace marking ignition ( ), beginning (↑) and end (↓) of fuel injection.

In **fig.3** the same data representation scheme was used as before. The only difference between the figures is that now the engine parameter "time of fuel injection during engine cycle" was changed. Where fig.2 showed images where fuel injection took place during the combustion stroke ("early" injection) the images of fig. 3 show distributions for fuel injection during the intake stroke ("late" injection).

The influence of this variation on the in-cylinder fuel distribution is clearly demonstrated in both upper images of the first row in fig.3 (single cycle and averaged). The speckled structure in the middle and the right of the images is due to spatially limited high fluorescence intensity of the fuel tracer which is synonymous with the existance of relatively big fuel droplets in the laser sheet volume. The size of the droplets was measured on the basis of the width at half maximum fluorescence intensity to be smaller than 600µm with high number density of big droplets. The existence of fuel droplets of this size inside the cylinder indicates that they are originating from fuel wall films on the intake valve and the intake port. The preferred appearence of the droplets at the right side of the image (close to the spark plug) is due to fluid mechanical conditions in the intake manifold and need further investigations. As expected the appearence of many fuel droplets results in smaller amounts of gaseous fuel in the cylinder during the intake stroke (compare the corresponding image of **fig.2**).

The influence of time of injection during the engine cycle is even still detectable in the compression stroke close to ignition (see images at 664°CA). The single cycle distribution still shows single not fully vapourized fuel droplets inside the cylinder and as well as the corresponding image in fig.2 a gaseous fuel distribution which is by far not uniform. Even in the averaged distribution single droplets are detectable and on average again higher fuel density could be registered in an area around the spark plug position.

The consequence of the detected bad vapourization and mixing of fuel with air can be seen in row three (4°CA) of **fig.3**. The single cycle snapshot image still shows nonuniformity of the fuel distribution. In addition the extention of the flame front is much smaller than in the image taken for injection during the combustion stroke. That this result is not only a statistical effect is clearly seen in the averaged image at the right. It turns out that on average at the same CA the flame front extention is much smaller for "late" fuel injection than for "early" injection (compare fig.2). This result is underlined by the corresponding averaged pressure trace at the bottom of fig.3. On average the IMEP for "late" injection in fig.3 is definitely smaller than for "early" injection in fig.2.

As discussed above cycle averaged fuel distribution images comprise valuable informations about basic fuel/air mixing- and combustion behaviour of SI-engines and the influence of engine parameter variations. For this reason in the following only cycle averaged images of the fuel distribution will be discussed.

In **fig.4** the influence of λ-value variation from stoichiometric (λ=1.0) to fuel rich (λ=0.8) is demonstrated. The left column displayes the averaged fuel distributions for an externally adjusted equivalence ratio of 1.0 for the already discussed CA and the right column represents the averaged distributions for an equivalence ratio of 0.8. In both cases fuel injection took place during the combustion stroke. In principle the general fuel distribution structures already described for fig 2 and 3 are reproduced for this parameter variation. On looking more carefully a higher fuel density is seen for the images taken for an equivalence ratio of 0.8. The result of higher equivalence ratio is shown in averaged images at 4°CA and the averaged pressure traces. The data show that on average and a fixed CA the flame front extends deeper into the cylinder volume for a λ-value of 0.8 than for a λ-value of 1.0. That means that the energy conversion during combustion takes place earlier and during a shorter period of time. Consequently the IMEP for fuel rich conditions is slightly higher than for stoichiometric mixtures.

Fig.5 shows consequences of exhaust gas recirculation (12%) on mixture formation and combustion (λ-value: 1.0, fuel injection during combustion stroke ("early")). For the experiments the exhaust gas was introduced into the intake manifold duct approximately 30 cm upstream the intake valve. The measurements show that with exhaust gas recirculation (EGR) higher amounts of gaseous fuel penetrate the cylinder in the early intake stroke (see 440°CA and CA°490). It is reasonable that this effect is caused by higher temperatures and therefore better evaporation of fuel due to the incoming hot exhaust gas. As can be seen in the combustion images at 710°CA this benefit for fuel evaporation is overcompensated by negative effects on the combustion reactions. It is easily seen in the images that the flame propagation in case without EGR is faster than with EGR. It should be noted, that the images were taken after a shorter delay (25°- 30° CA) past ignition than the images in fig.2-4 (40° 45° CA). In the left column (without EGR) the flame has already reached the measurement volume while in the right column (with EGR) the flame is so slow that it has not yet reached the laser sheet.

The effects of EGR are particularly obvious in the averaged pressure traces displayed below the images. While the pressure trace without EGR show a normal course, the trace for activated EGR is strongly flattened and indicates retarded inflammation.

Beside these averaged qualitative informations about in cylinder fuel distributions and flame propagation also quantitative data can be derived from the raw images. In order to convert the measured fluorescence intensities to

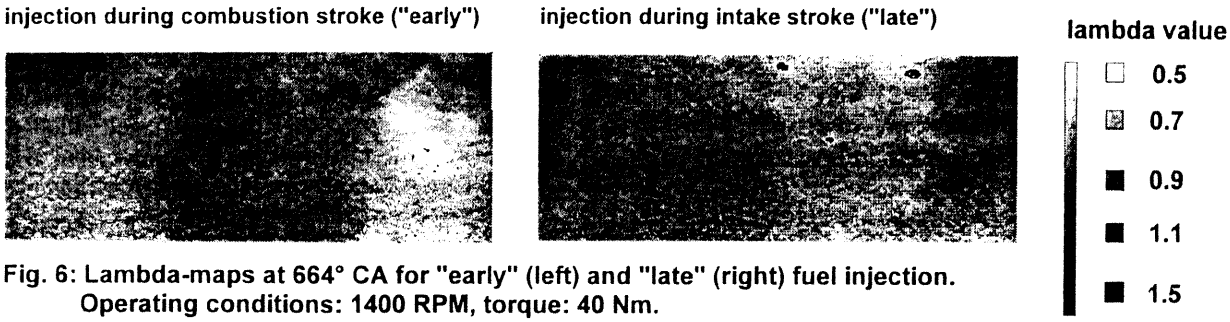

Fig. 6: Lambda-maps at 664° CA for "early" (left) and "late" (right) fuel injection. Operating conditions: 1400 RPM, torque: 40 Nm.

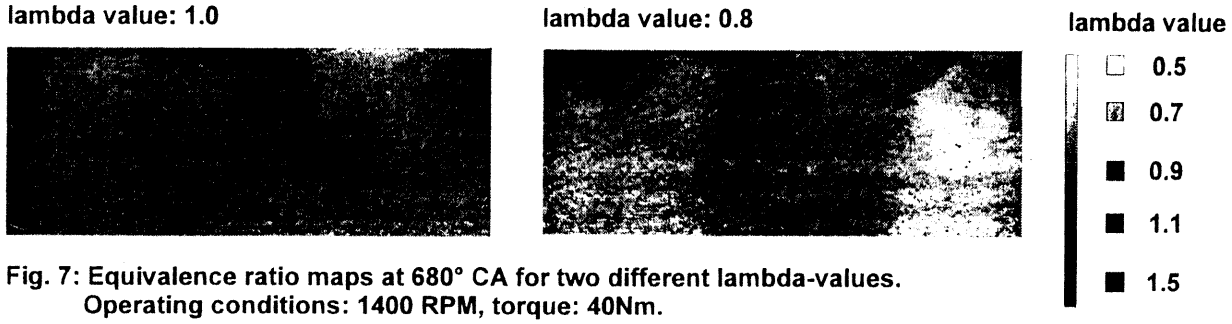

Fig. 7: Equivalence ratio maps at 680° CA for two different lambda-values. Operating conditions: 1400 RPM, torque: 40Nm.

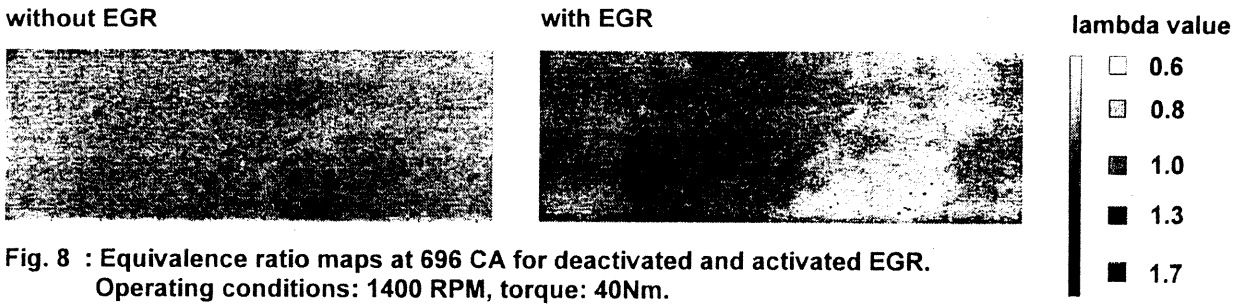

Fig. 8 : Equivalence ratio maps at 696 CA for deactivated and activated EGR. Operating conditions: 1400 RPM, torque: 40Nm.

lambda values a simple calibration procedure was applied:

1. Few CA before ignition cycle averaged (20 cycles) fuel tracer fluorescence images were recorded.

2. It is assumed that for this CA at the end of the compression stroke the turbulent mixing of fuel and air is far advanced and therefore the cyclic and spatially averaged fluorescence intensity represents the mean fuel density of the whole cylinder volume.

3. Then this averaged fluorescence intensity is identified with the equivalence ratio measured by a lambda probe (Bosch LSM11 0258104001) in the exhaust manifold so that every fluorescence intensity now corresponds explicit to a defined equivalence ratio.

4. Assuming identical conditions (gas temperature, pressure) this calibration procedure now permits the quantification of single cycle snap shot images of the relative fuel density. Some results of this calibration are presented in **figure 6-8**. Here the pure qualitative information about relative fuel density distribution is converted to equivalence ratio maps. The error resulting from measurement and calibration procedure is estimated to be 10%.

In **figure 6** two equivalence ratio maps for 664°CA are shown which correspond to the single cycle fuel distribution images presented in figure 2 and 3 (variation of time of injection during the engine cycle). For these images the grey values represent λ-values as indicated at the right. It should be noted that the three black dots in the image taken for injection during the intake stroke represent fuel droplets so that their λ-value cannot be represented by the actual scale. The preadjusted λ-value (measured by the λ-probe) for the images of figure 6 was 0.8. In both images strong equivalence ratio variations from 0.5 up to 1.1 are observable.

In **figure 7** single cycle λ-value-maps at 680°CA for external variation of the overall λ-value are displayed. It can be seen that the occurring λ-variations are in the same regime than those in figure 6.

The results of the variation of the exhaust gas recirculation status is demonstrated in **figure 8** (externally adjusted λ-value was 1.0). Note that the λ-value scale at the right has changed. As already known from earlier experiments the small black dots in the images are artificial and result from oil dirtying on the piston window. Obviously stronger λ-value variations ocure in case of activated exhaust gas recirculation (λ=0.6 to λ= 1.6)

SUMMARY AND CONCLUSION

The present work demonstrates that 2D-LIF measurements of relative fuel density distributions in modified mass production SI engines are possible and reveal deep insight in the turbulent fuel/air mixing process inside the cylinder. Planar fuel distributions were observed for selected crank angles in the intake, compression and combustion stroke. Snap shot images of the distributions clearly show local variations of fuel density and are convertable to λ-value maps. Cycle averaged images reveal recurring distribution structures and reveal the general influence of engine parameter variations. Variation of the engine parameters time of injection, λ-value and exhaust gas recirculation were carried out and the in-cylinder measurement of averaged fuel distributions clearly show the resulting changes of fuel distribution and the influence on flame propagation. The new insights in mixing formation and combustion resulting from parameter variations in correlation with the resulting effects on flame propagation and IMEP show strong relevance to real mass production engines. For example it turned out that for the present experimental conditions fuel injection during the intake stroke results in slow energy conversion and therefore low IMEP due to droplet penetration into the cylinder.

In addition to the qualitative informations about spatial fuel distributions quantitative 2D λ-value maps could be derived using simple calibration procedures. It turned out, that single combinations of the engine parameters result in strong air/fuel ratio variations.

REFERENCES

1. Dyer, T.M., "New Experimental Techniques for In-Cylinder Engine Studies", SAE Paper No. 850396, 1985.
2. Grünefeld, G., Beushausen, V., Andresen, P., Hentschel, W., "Spatially Resolved Raman Scattering for Multi-Species and Temperature Analysis in Technically Applied Combustion Systems: Spray Flame and Four-Cylinder In-Line Engine", submitted to Appl. Phys B.
3. Eckbreth, A.C., "Laser Diagnostics for Combustion Temperature and Species", Abacus Cambridge MA, 1988.
4. Andresen, P., Meijer, G., Schlüter, H., Voges, H., Koch, A., Hentschel, W., Oppermann, W., Rothe, E., "Fluorescence imaging inside an internal combustion engine using tunable excimer lasers", Appl. Opt. **29**,16 2392-2404, 1990.
5. Koch, A., Voges, H., Andresen, P., Schlüter, H., Wolff, D., Hentschel, W., Oppermann, W., Rothe, E., "Planar Imaging of a Laboratory Flame and of Internal Combustion in an Automobile Engine using UV Rayleigh and Fluorescence Light", Appl. Phys. B **56**, 177-184, 1993.
6. Hanson, R. K. "Combustion Diagnostics: Planar Imaging Techniques" Twenty-first Symposium (International) on Combustion/The Combustion Institute, Pittsburgh, pp.1677-1691, 1992.
7. Arnold, A., Becker, H., Suntz, R., Monkhouse, P., Wolfrum, J., Maly, R., Pfister, W., " Flame Front Imaging in an Internal-Combustion Engine Simulator by Laser-Induced Fluorescence of Acetaldehyde", Opt. Lett. 15, pp. 831-833, 1990
8. Grünefeld, G., Beushausen, V., Andresen, P., Hentschel, W., "A Major Origin of Cyclic Energy Conversion Variations in SI Engines: Cyle-by-Cycle Variations of the Equivalence Ratio and Residual Gas of the Initial Charge.", submitted to the SAE-Meeting "Fuels and Lubricants", Baltimore 1994.
9. Lawrenz, W., Köhler, J., Meier, F., Stolz, W., Wirtz, R., Bloss, W. H., Maly, R. R., Wagner, E., Zahn, M., Zahn, "Quantitative 2D LIF Measurements of Air/Fuel Ratios During the Intake Stroke in a Transparent SI Engine", SAE-paper No. 922320, San Francisco, 1992.
10. Lozano, A. Yip, B., Hanson, R. K., "Acetone: a tracer for concentration measurements in gaseoous flows by planar laser-induced fluorescence", Exp. in fluids 13, pp.369-376, 1992.
11. Sohma, K., Yukitake, T. Azuhato, S., Takaku, Y., "Application of Rapid Optical Measurement to Detect the Fluctuations of the Air-Fuel Ratio and Temperature of a Spark Ignition Engine", SAE-paper NO. 910499.
12. Shimizu, R., Matumoto, S., Furuno, S., Murayama, M., Kojima, S., "Measurement of Air-Fuel Mixture Distribution in a Gasoline Engine Using LIEF Technique", SAE-paper, San Francisco, 1992.
13. Vannobel, F., Arnold, A., Buschmann, A., Cousyn, B., Decker, M., Sick, V., Wolfrum, J., "Simultaneous Imaging of Fuel and Hydroxyl Radicals in an In-Line Four Cylinder SI Engine." SAE-paper No. 932696, 1993